Resolution of the Apparent Disorder of the Rb_2 $A^1\Sigma_u^1(0_u^+)$ and $b^3\Pi_u(0_u^+)$ Spectra: A Case of Fully Coupled Electronic States

C. Amiot, O. Dulieu, and J. Vergès

*Laboratoire Aimé Cotton, CNRS II, Bâtiment 505, Campus d'Orsay, 91405 Orsay cedex, France**

(Received 20 January 1999)

Strong perturbation effects in the infrared fluorescence spectra recorded after the resonant excitation process $X^1\Sigma_g^+ \rightarrow A^1\Sigma_u^+(0_u^+) \rightarrow (2)^1\Pi_g$ in Rb_2, have been observed by high resolution Fourier transform spectroscopy. They arise from complete coupling of the two states over the whole range of binding energies, yielding unusual molecular spectra with oscillating vibrational and rotational structures. A quantitative interpretation, based on Fourier grid Hamiltonian method calculations, of these newly observed phenomena is given. This opens new opportunities to study the triplet manifold in Rb_2, RbCs, and Cs_2, particularly the lowest state relevant for precise scattering length determination.

PACS numbers: 33.20.Ea, 31.15.Qg, 33.20.Vq

Interaction between two electronic states becomes important when constants of motion are nearly degenerate and when the total angular momentum J of the levels are equal [1]. One of the most obvious effects of these interactions is the perturbation of the regularity of the rovibrational structure. In alkali dimers, the first excited $A^1\Sigma_u^+(0_u^+)$ and $b^3\Pi_u(0_u^+)$ electronic states, represented in Fig. 1, are a long known example of such singlet-triplet interactions. As far back as 90 years ago, Wood [2] showed that the magnetic rotation spectrum of Na_2 contained anomalies localized in energy, that were later demonstrated to arise from spin-orbit perturbations of the $A^1\Sigma_u^+(0_u^+)$ state by the $b^3\Pi_u(0_u^+)$ state [3].

A great deal of work has been devoted to the spectroscopic studies of these two states for the lightest alkali dimers Li_2 [4], Na_2 [5], and K_2 [6]. The A and b spin-orbit interactions have been the subject of several high-resolution laser spectroscopic studies [7]. Elaborate deperturbation procedures were used only in restricted energy ranges, in order to extract from the observations, molecular constants, and estimated coupling parameters between unperturbed electronic states.

The spin-orbit interaction strongly increases from lithium to cesium, since the splitting ΔE_{fs} of the ^2P atomic level grows from 0.34 to 554.1 cm^{-1}, respectively. The intensity of the mixing between singlet and triplet states grows by spoiling the spin quantum number. As a consequence, it is needed to consider the two states as fully coupled ones, requiring specific theoretical methods to characterize them [8].

In this Letter, we report on the Rb_2 $(2)^1\Pi_g \rightarrow$ (A and b) infrared fluorescence recorded at high resolution by Fourier transform spectroscopy (FTS), showing that almost all the rovibrational levels of both states are perturbed regardless of their energy spacing, leading to a previously not reported chaotic appearing energy level structure. Such a feature provides the opportunity to open large windows for perturbation facilitated multiple resonance spectroscopy, allowing detailed studies on the almost unknown triplet manifold in Rb_2.

The experiment has been previously described in our Rb_2 $B^1\Pi_u$ state study [9]. Briefly, Rb_2 molecules produced at 300 °C in a stainless-steel heat-pipe oven, are excited by a cw tunable Ti:sapphire laser (Coherent 899-21), operated with middle wavelength optics. Optical-optical double resonance is used to populate the $(2)^1\Pi_g$ electronic state. Fluorescence is observed down to the $B^1\Pi_u$ state [9] and also to the $A^1\Sigma_u^+(0_u^+)$ state.

Examples of recorded spectra [two Q and one (P, R) spectra] are displayed in Fig. 2 as functions of the transition wave number, for three of the transitions summarized in Table I. Figure 2a depicts the case where a level of the A state with $J' = 69$ and $E' = 11\,582.862$ cm^{-1} in $^{85}Rb_2$ is populated from the ground state level ($v'' = 0$, $J'' = 70$, $E'' = 139.730$ cm^{-1}). The $(2)^1\Pi_g$ f sublevel at $E = 23\,025.993$ cm^{-1} is subsequently populated. The fluorescence series marked on the figure corresponds to ($A \sim b$) levels with rotational quantum number $J = 69$. Fifteen Q lines labeled from 0 to 14 are observed: they

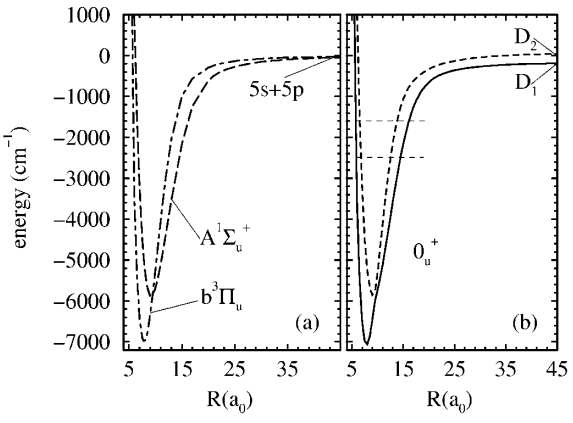

FIG. 1. Potential curves of the $A^1\Sigma_u^+(0_u^+)$ and $b^3\Pi_u(0_u^+)$ electronic states in Rb_2: (a) in Hund's case a, from Refs. [10,11]; (b) in Hund's case c after diagonalization of the atomic spin-orbit interaction. Horizontal dashed lines in (b) figure the energy range explored in the experiment. D_1 and D_2 hold for the $5^2S + 5^2P_{1/2}$ and $5^2S + 5^2P_{3/2}$ dissociation limits, respectively.

 0031-9007/99/83(12)/2316(4)$15.00 © 1999 The American Physical Society

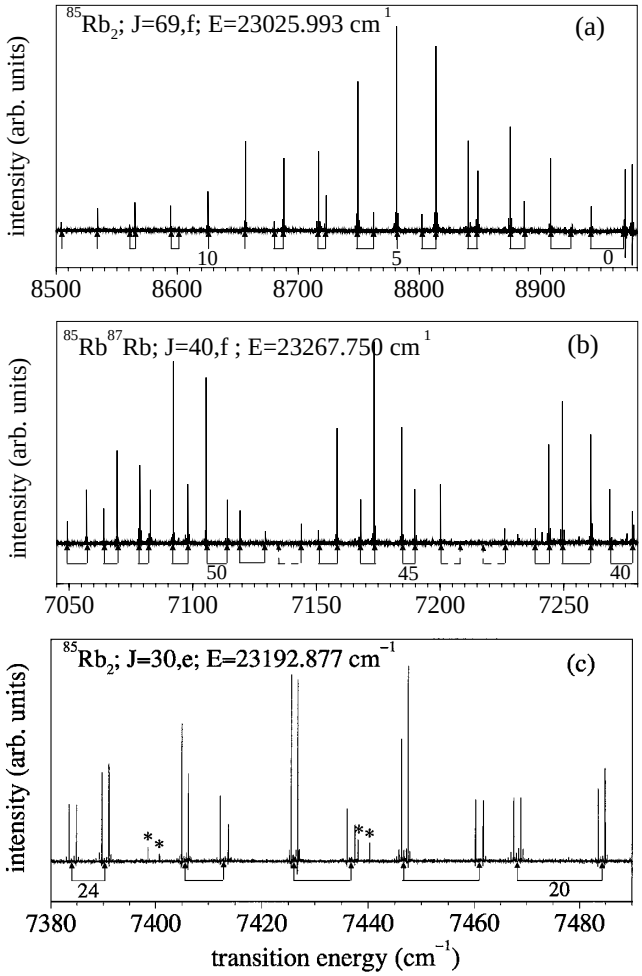

FIG. 2. Pieces of Fourier transform fluorescence spectra for the transition $(2)^1\Pi_g(J;E) \rightarrow (A^1\Sigma_u^+$ and $b^3\Pi_u)$ in Rb_2. The energy E and rotational quantum number J of the initial level are reported in each case. The labeling of the levels refers to the complete series of lines identified in the spectra. In (a) and (b), most of the Q lines are arranged in doublets. Broken arrows in (b) show the predicted position of missing lines, according to our theoretical model. In (c) pairs of P and R lines are also arranged in doublets. Stars indicate lines corresponding to the fluorescence towards the $B^1\Pi_u$ state [9].

are associated with a vibrational series having an irregular spacing. Some weaker "extra lines" appear, arranged in doublets with an intense component. This is a typical case of localized perturbations between A and b levels: due to selection rules, the fluorescence transition involves the A component of the wave function of the mixed $(A \sim b)$ levels, and produces a single line (like lines 5, 9, 10, 13, 14) for unperturbed levels, and doublets of lines for perturbed levels. The most intense perturbations occur for lines 3 and 7, where intensities within the doublet are similar. This manifests clearly in the progression of the absolute $(A \sim b)$ term energy values T_e, obtained by substracting the upper state energy from the observed line wave numbers. They are located between 14 084.06 and 14 552.02 cm^{-1}, and represented in Fig. 3, after substraction of the average energy value T_e^{moy} on the considered energy range. The structure, although irregular, is not very different from those observed in lighter alkalis Na_2 and K_2.

Consider now the case of a higher $(2)^1\Pi_g$ level $(J = 40, f)$ pumped at $E = 23\,267.750$ cm^{-1}, in the $^{85}Rb^{87}Rb$ molecule. The fluorescence spectrum in Fig. 2b shows that each Q line splits in a doublet of lines with irregular spacing. More than 50 doublets are observed, with energy ranging between 15 238.64 and 16 231.77 cm^{-1}. The derived spacing between the first line of two consecutive doublets (see Fig. 4), depicts an oscillating structure of the spectrum which cannot with certainty be associated to a single unperturbed electronic state. The spacing between the two lines of the same doublet is also plotted in Fig. 4, and exhibits also oscillations.

The last example concerns a situation where in an unperturbed case, doublets of P, R lines are expected. The $J = 30, e$ level of $(2)^1\Pi_g$ at $E = 23\,192.877$ cm^{-1} in $^{85}Rb_2$ is populated, and part of the resulting fluorescence spectrum is displayed in Fig. 2c. The complete results give 29 doublets, located between 15 194.54 and 15 896.50 cm^{-1}. It exhibits a series of doublets of (P, R) pairs with different relative intensities. A similar analysis of the line spacings, not reported here, shows oscillations as in the previous case (Fig. 4). The energy spacing Δ_{PR} between P and R lines of each doublet is related to the rotational constant B_v of the corresponding level, according to $\Delta_{PR} = B_v(J + 1)(J + 2) - B_v(J - 1)J = 4B_v(J + 1/2)$, and is plotted in Fig. 5. The nature of the vibrational levels is clearly oscillating between two patterns, depending on its fraction of A and b characters.

The above examples clearly show that the usually observed regularity of molecular spectra associated with isolated and well-behaved potential curves cannot be expected for this system. Actually, three other experimental spectra (specified in the last three lines of Table I but not displayed here) confirm this pattern, and will be discussed in a further paper. It is worth noting that a strong difficulty arises in the line assignments: the energy spacing between Q lines or a (P, R) pair of lines within a given doublet can be of the same magnitude as the energy spacing between two successive doublets.

In order to provide an unambiguous attribution of these lines, we have performed theoretical calculations of the rovibrational bound levels of the coupled A and b Rb_2 electronic states, in the framework of the Fourier grid Hamiltonian (FGH) method. A detailed description of this method can be found elsewhere [8]. Such an approach is particularly well suited for our purpose, due to its global noniterative character: all eigenvalues of the coupled system are deduced from the diagonalization of a $(pN) \times (pN)$ square matrix, where p is the number of coupled states, and N the number of grid points used to represent the interatomic distance range of interest. The

TABLE I. Double resonance absorption transitions yielding the fluorescence spectra studied in the present work. Only the spectra corresponding to the first three transitions are displayed in figures.

	$X^1\Sigma_g^+$			$A^1\Sigma_u^+$		$(2)^1\Pi_g$	
	v''	J''	$E''(\mathrm{cm}^{-1})$	J'	$E'(\mathrm{cm}^{-1})$	J	$E(\mathrm{cm}^{-1})$
$^{85}Rb_2$	0	70	139.730	69	11 582.862	69, f	23 025.993
$^{85}Rb_2$	0	28	47.017	29	11 619.947	30, e	23 192.877
$^{85}Rb^{87}Rb$	1	39	120.254	40	11 694.002	40, f	23 267.750
$^{85}Rb_2$	0	9	30.871	8	11 604.619	7, e	23 178.367
$^{85}Rb_2$	0	73	149.336	72	11 706.073	72, f	23 262.810
$^{85}Rb_2$	0	81	176.881	82	11 735.046	82, f	23 293.211

$N \times N$ diagonal blocks map the kinetic and potential energy operators for each of the p coupled states, while the $N \times N$ off-diagonal blocks map the coupling operators.

The computations were done using the most accurate available Rb_2 potential curves [10] between $5a_0$ and $20a_0$ ($1a_0 = 0.0529$ nm), matched to asymptotic curves from Ref. [11], and dissociating to the experimental atomic dissociation limit $5s + 5p$. Neglecting the coupling between the rotation of the molecule and the total electronic momentum, we restrict our model to the two A and b states, interacting through a constant spin-orbit coupling $V_{so} = \sqrt{2}\,\Delta E_{fs}/3 = 112\ \mathrm{cm}^{-1}$. The contribution of the rotation is added as a diagonal $J(J+1)/2\mu R^2$ term, where μ is the reduced mass of the system ($\mu = 77\,392.3761$, 78 292.0476, and 79 212.8822 a.u. for the three species $^{85}Rb_2$, $^{85}Rb^{87}Rb$, and $^{87}Rb_2$, respectively [12]).

The domain of internuclear distances covered by the wave functions of the observed levels can be determined by estimating the corresponding range of their binding energy E_v (with respect to the $5^2S + 5^2P_{1/2}$ asymptote), according to $E_v = E - E_v^{\mathrm{fluo}} - D_e^X - E_{D_1}$. In this formula, $D_e^X = 3993.530(60)\ \mathrm{cm}^{-1}$ is the well depth of the Rb_2 ground state [13], $E_{D_1} = 12\,578.9484\ \mathrm{cm}^{-1}$ is the energy of the D_1 atomic transition [14], E is the energy of the populated $(2)^1\Pi_g$ level, and E_v^{fluo} represents the fluorescence energy. The observed levels are bound by energies located between 2500 and 500 cm^{-1}, restricting the vibrational motion (for $J = 0$ levels) to internuclear distances between $5a_0$ and $20a_0$ (see Fig. 1). A uniform grid of about 700 points is required to describe properly the coupled states over this distance range, according to the relation between the largest possible grid step δx and the maximum momentum $k_{\max}$ involved in the system: $\delta_x = \pi/(2k_{\max})$ [8]. Diagonalization of 1400×1400 squared matrices has been required. We have further checked the accuracy of the present results with the newly developed mapped FGH method [15], which implies a variable grid step reducing the number of grid points to about 500 points.

The agreement between our model and experimental results is surprisingly good, as demonstrated in Figs. 4 and 5: no more than a few percent shift is found in the line energy differences. In several cases, predictive calculations helped for an unambiguous attribution of lines, when the spacing between different doublets on one hand, and between the components of a given doublet

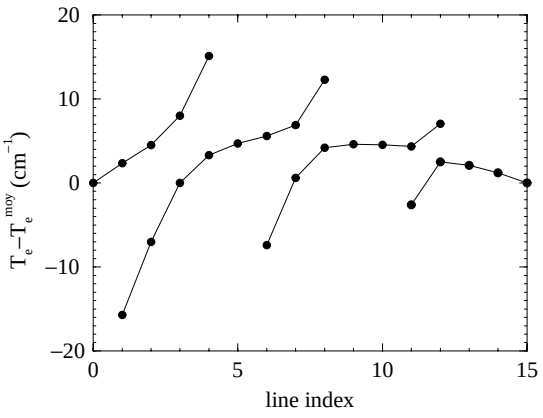

FIG. 3. Absolute term energy values of the mixed (A and b) levels shown in Fig. 2a, after substraction of the mean term energy value. The line index refers to the labeling of the spectrum. Lines are drawn for clarity.

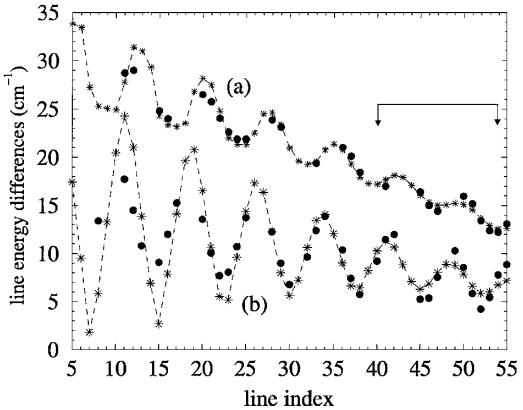

FIG. 4. Energy spacing between (a) the first component of consecutive doublets, (b) components of the same doublet, corresponding to spectrum of Fig. 2b. The range of the displayed spectrum is indicated with arrows, and the same labeling is used (beginning arbitrarily at 8 for the first observed line). Both experimental (full circles) and calculated (stars) results are shown. The dashed line is drawn for guiding the eye.

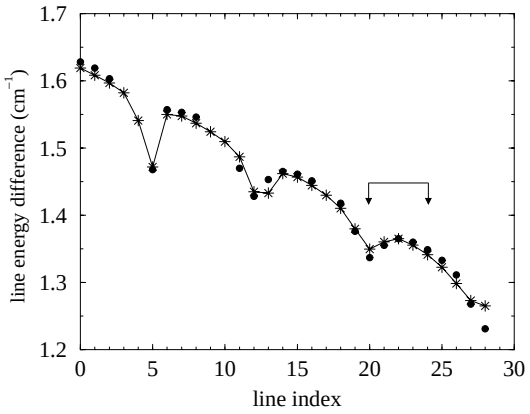

FIG. 5. Energy spacing of P and R lines corresponding to spectrum of Fig. 2c. The range of the displayed spectrum is indicated with arrows, and the same labeling is used. Both experimental (full circles) and calculated (stars) results are shown. The dashed line is drawn for guiding the eye.

on the other hand were comparable. It allowed us also to predict missing (pure triplet) lines in doublets labeled 43, 44, and 48 of Fig. 2b (identified by broken arrows). Such a good agreement can be interpreted if we invoke the following argument: for the quite highly excited vibrational levels studied here, the main contribution to the energy comes from the outer turning point of the potential curves, located at distances (between $15a_0$ and $20a_0$) where the assumption of the atomic spin-orbit coupling is certainly correct. Moreover, this confirms the high quality of the potential curves of Foucrault *et al.* [10] in this range of distances, well outside the region where core-core effects are important, and yielding an accurate spacing between energy level. However, a similar agreement was not obtained in the first spectrum of Fig. 2a, probably due to the fact that it involves deeper levels for which the above assumptions begin to fail.

We have been able to observe similar apparently disordered spectra for three other double resonance transitions, which are not reported here. Their treatment is currently under progress. Another feature which could also help both for the attribution of the lines, and for the test of potential curves, is the relative intensities of lines belonging to the same doublet, which could be related in a first approximation to the amount of A or b state character in the coupled state calculations.

Finally, the search for this type of perturbations in other heavy alkali systems like RbCs or Cs_2 is presently under investigation in our laboratory. As stated above, this particular behavior of the heavier alkali dimers provides the opportunity to investigate their almost unknown triplet manifold over large energy windows, through multiple resonance spectroscopy. Fluorescence back to the lowest $a^3\Sigma_u^+$ may yield crucial information for the determination of scattering length [16] in these species.

V. Kokoouline is gratefully acknowledged for his help in using the mapped Fourier grid Hamiltonian code.

*Laboratoire Aimé Cotton is associated with the Université Paris-Sud.

[1] H. Lefebvre-Brion and R. W. Field (Academic, New York, 1986).
[2] R. W. Wood and F. E. Hackett, Astrophys. J. **30**, 339 (1909).
[3] R. S. Mulliken, Rev. Mod. Phys. **4**, 15 (1932); W. R. Fredrickson and C. R. Stannard, Phys. Rev. **44**, 632 (1933); T. Carroll, Phys. Rev. **52**, 822 (1937).
[4] P. Kusch and M. M. Hessel, J. Chem. Phys. **67**, 586 (1977); C. Linton *et al.,* J. Mol. Spectrosc. **175**, 340 (1996); C. Linton *et al.,* J. Mol. Spectrosc. **151**, 159 (1992); K. Urbanski *et al.,* J. Chem. Phys. **104**, 2813 (1996).
[5] W. T. Luh *et al.,* J. Mol. Spectrosc. **111**, 327 (1985); Li Li *et al.,* J. Mol. Spectrosc. **105**, 344 (1984); H. G. Krämer *et al.,* Chem. Phys. Lett. **272**, 391 (1997).
[6] A. M. Lyyra *et al.,* J. Chem. Phys. **92**, 43 (1990); B. Ji *et al.,* J. Chem. Phys. **102**, 6646 (1995).
[7] C. Effantin *et al.,* J. Phys. B **18**, 4077 (1985); G. Jong *et al.,* J. Mol. Spectrosc. **155**, 115 (1992); A. M. Lyyra *et al.,* in *Advanced Series in Physical Chemistry: Molecular Dynamics and Spectroscopy by Stimulated Emission Pumping,* edited by H.-L. Dai and R. W. Field (World Scientific, Singapore, 1995), p. 459; Li Li and R. W. Field, *ibid.,* p. 251.
[8] R. Kosloff, J. Phys. Chem. **92**, 2087–2100 (1988); O. Dulieu and P. S. Julienne, J. Chem. Phys. **103**, 60 (1995).
[9] C. Amiot and J. Vergès, Chem. Phys. Lett. **274**, 91 (1997).
[10] M. Foucrault *et al.,* J. Chem. Phys. **96**, 1257 (1992).
[11] M. Marinescu and A. Dalgarno, Phys. Rev. A **52**, 311 (1995).
[12] I. Mills *et al.,* in *Quantities, Units and Symbols in Physical Chemistry* (Blackwell Scientific Publications, Oxford, England, 1993), 2nd ed.
[13] C. C. Tsai *et al.,* Phys. Rev. Lett. **79**, 1245 (1997).
[14] G. P. Barwood *et al.,* Appl. Phys. B **53**, 142 (1991).
[15] V. Kokoouline, O. Dulieu, R. Kosloff, and F. Masnou-Seeuws, J. Chem. Phys. **110**, 9865 (1999).
[16] H. M. J. M. Boesten *et al.,* Phys. Rev. A **55**, 636 (1997); Ph. Courteille *et al.,* Phys. Rev. Lett. **81**, 69 (1998); J. L. Roberts *et al.,* Phys. Rev. Lett. **81**, 5109 (1998).